Published by :
http://www.ijert.org

International Journal of Engineering Research & Technology (IJERT)
ISSN: 2278-0181
Vol. 13 Issue 9, September 2024

Thermal Analysis and Generalized Cattaneo-Christov Concept in Stagnation Point Maxwell Nanofluid Flow with Chemical Reaction and Variable Thermal Conductivity

Mowffaq Oreijah
Mechanical Engineering Department, College of Engineering and Architecture,
Umm Al-Qura University, P. O. Box 5555, 21955 Makkah, Saudi Arabia

M. Ijaz Khan
Department of Mechanical Engineering, College of Engineering,
Prince Mohammad Bin Fahd University, Al-Khobar, Saudi Arabia

K. Karthik
Department of Studies in Mathematics, Davangere University,
Davangere, Karnataka, 577002, India

Nainaru Tarakaramu
Department of Mathematics, School of Liberal Arts & Sciences, Mohan Babu University,
Sree Sainath Nagar, Tirupati-517102, Andrapradesh, India
Department of Mathematics, Humanities and Basic Science,
Sree Vidyanikethan Engineering College,
Tirupati-517102, Andrapradesh, India

Dilsora Abduvalieva
Department of Mathematics and Information Technologies,
Tashkent State Pedagogical University,
Bunyodkor Avenue, 27, Tashkent, 100070, Uzbekistan

Manish Gupta
Division of Research and Development,
Lovely Professional University, Phagwara, India

Abstract: **The present study discusses the Cattaneo-Christov mass and heat fluxes in the stagnation point flow of Maxwell nanoliquid. The stream is created due to the extending of a cylinder. Solutal and thermal convective conditions are imposed. Heat and mass transportation characteristics are discussed by employing the Cattaneo-Christov fluxes theory. Brownian motion, chemical reaction, and thermophoresis features are discussed. Energy relation comprises radiation and heat generation. Governing nonlinear partial differential systems are altered into non-dimensional ordinary systems (ODEs) by suitable transformation. The homotopic analysis technique (HAM) is employed to develop convergent solutions. Graphical results illustrating the influence of various emerging parameters on concentration, liquid flow and thermal field. Here, it is concluded that for higher material parameters, velocity decays. Higher estimation of thermal and solutal Biot numbers increases both concentration and thermal field. An intensification in temperature is detected for thermal conductivity and heat generation parameters.**

Keywords*:* **Maxwell fluid model; Cattaneo-Christov flux models; Thermal radiation; Heat source; Chemical reaction and variable thermal conductivity.**

International Journal of Engineering Research & Technology (IJERT)
ISSN: 2278-0181
Vol. 13 Issue 9, September 2024

Nomenclature:

u, v **velocity components [** $m\,\sec^{-1}$ **]**	x, r **cylindrical coordinates [** m **]**
$\alpha^* = \frac{k_f}{(\rho c_p)_f}$ **thermal diffusivity [** $m^2\,\sec^{-1}$ **]**	ν_f kinematic viscosity [$m^2\,\sec^{-1}$]
h_f , h_w **heat and mass transfer rates**	l reference length [m]
ρ_f **density [** kgm^{-3} **]**	D_t thermophoresis coefficient [$m^2\,\sec^{-1}$]
$(c_p)_f$ **specific heat [** $Jkg^{-1}K^{-1}$ **]**	$\Pr$ Prandtl number
λ_1 **relaxation time**	$\in$ variable thermal conductivity parameter
T_w **wall temperature [** K **]**	a , c reference velocities [$m\,\sec^{-1}$]
τ **ratio of heat capacities**	λ_c solutal relaxation time
Re_x **local Reynold number**	T_∞ ambient temperature [K]
ω **curvature variable**	C concentration
k_f **thermal conductivity [** $Wm^{-1}K^{-1}$ **]**	Sc Schmidt number
R **Radius of cylinder [** m **]**	σ^* Stefan-Boltzmann constant [$Wm^{-2}K^{-4}$]
δ_C **solutal relaxation time**	Rd radiation variable
k_r **reaction rate [** $\sec^{-1}$ **]**	α_t thermal relaxation time variable
C_∞ **ambient concentration**	Nb random motion variable
A **stretching ratio variable**	λ_t heat relaxation time
D_b **Brownian motion coefficient [** $m^2\,\sec^{-1}$ **]**	T temperature [K]
C_w **wall concentration**	Nu_x Nusselt number
α_1 **Maxwell fluid parameter**	$Q > 0$ heat generation variable
$Q_0 > 0$ **heat generation coefficient**	k^* mean absorption coefficient [m^{-1}]
τ_{xr} **wall shear stress**	γ reaction variable
q_w , j_w **heat and mass flux**	Sh_x Sherwood number
Nt **thermophoresis parameter**	γ_1 , γ_2 thermal and solutal Biot numbers
α_c **solutal relaxation time variable**	

International Journal of Engineering Research & Technology (IJERT)
ISSN: 2278-0181
Vol. 13 Issue 9, September 2024

1: INTRODUCTION

There is a growing attention in studying the motion of non-Newtonian fluids in boundary layers because of their many practical uses in manufacturing and industrial procedures. Some examples of these uses include drilling muds, polymer plastics, optical fibres, hot-rolling paper manufacture, metal spinning, and chilling metal plates in cooling baths. Researchers have previously put out a variety of non-Newtonian models, as no one model can account for all the characteristics of non-Newtonian resources. Three main categories may be used to group these models: differential, rate, and integral-type fluids. The liquid model being discussed is a specific form of rate-type fluid called a Maxwell fluid. This model, based on fluid dynamics, predicts the effects of relaxation time. The behavior of differential-type fluids does not allow for accurate prediction of such effects. The properties of a Maxwell fluid exhibit a viscous flow over extended periods of time while simultaneously displaying additional elastic resistance to sudden deformations. The phenomenon seen is stress relaxation, which is the gradual decrease in tension over time under persistent pressure. It lacks creep, indicating that the deformation does not progressively grow over time under steady pressure. The Maxwell liquid model is a basic representation of viscoelasticity that may effectively depict key characteristics of real fluids, including stress reduction and elastic confrontation. Megahed [1] examined the heat transfer enhancement process through a Maxwell liquid motion across an extending sheet. Olabode et al. [2] explored the effect of quadratic convection on the Maxwell liquid motion via a permeable media utilizing the collocation technique. Kumar et al. [3] considered behavior of CNTs based magnetic dipole movement in flow of Maxwell flow towards a moving surface. With the thermal flux, Khan et al. [4] elucidated the Maxwell fluid motion across an inclined plate using the natural convection computation. The significance of heat generation on the Maxell liquid stream via a sensor sheet was delineated by Salahuddin et al. [5].

The thermal boundary layer refers to a narrow region around an object that characterizes the interactions between fluid flow and thermal processes. The heat of the fluid rises inside the temperature boundary layer as it flows around a heated object, leading to an upsurge in heat transport and a subsequent enhancement of transport spectacles by reducing the viscosity of the fluid. Thermal radiation is crucial in several manufacturing processes that function at high temperatures, such as gas turbines, nuclear reactors, and other propulsion systems. Furthermore, thermal radiation is a crucial factor in the heat transportation properties of fluids that absorb and release heat, especially in situations when heat transfer via convection is minimal, such as in free convection difficulties. Currently, the control of the temperature in the human bloodstream using thermal radiation is crucial in numerous medical therapies for conditions such as muscular spasms, myalgia, persistent widespread pain, and irreversible muscle shortening. Furthermore, it has comparable significance in several biomedical engineering applications and various thermal therapeutic techniques. Kumar et al. [6] studied the significance of radiation on the temperature dispersal of the concave fin under periodic boundary circumstances. Kumar et al. [7] analyzed the heat transfer features of the nanofluid flow via a vertical surface with radiation. The study showed by Yu et al. [8] absorbed on examining the optimal effects of fluid convection influenced by carbon nanotubes and thermal radiation. The flow of Carreau fluid via a stretching sheet under the influence of thermal radiation was elaborated by Lim et al. [9]. Albalawi et al. [10] probed the effect of thermal radiation on the motion of nanofluid via a coaxial cylinder under nanoparticle aggregation.

Heat transport is a common phenomenon in nature due to thermal differences between things or inside the same body. Fourier formulated an established rule of heat conduction that provides a means to inspect the analysis of heat transport. Cattaneo improved Fourier's law of heat conduction by including the concept of relaxation time to address inconsistencies in heat conduction. In light of this, Christov developed a time-derivative heat flux model known as the Cattaneo-Christov (C-C) model, which is highly helpful for the study of convective heat transfer. Using this perspective, many scholars have used the C-C heat flux model to demonstrate magnetohydrodynamic flow as well as heat transfer and have also concluded that the heat transport rate can be increased by enhancing the thermal relaxation time. Using the C-C model, Gowda et al. [11] assessed the stream of non-Newtonian liquid via a flat surface under the radiation impact. Gowda et al. [12] examined the effect of the C-C heat flux model on the Sutterby nanofluid stream across a stretchy disk. Jawad and Nisar [13] assessed the flow of Maxwell fluid past a porous surface near the magnetohydrodynamic stagnation point in the presence of C-C heat flux model. Hussain and Mao [14] used the C-C heat flux model to study the Prandtl-Eyring fluid flow over a variable stretching sheet. Li et al. [15] investigated Darcy-Forchheimer based bio-convective periodically accelerated flow of non-Newtonian materials subject to CC model and Prandtl effective approach.

The heat transportation reflections observed in large environments vary from the outcomes gained in the performance of a heat source/sink (H-SS). Therefore, the H-SS is located within small inclusions to achieve efficient control processes on the heat transport properties of different contemporary electric products. This particular type of H-SS is

International Journal of Engineering Research & Technology (IJERT)
ISSN: 2278-0181
Vol. 13 Issue 9, September 2024

often used to regulate temperature in some fundamental components of electrical structures. The majority of the existing work on heat transport research primarily focuses on the impact of temperature-dependent H-SS. This is because the temperature-dependent H-SS is often used to regulate the mass and heat transfer properties of the liquid. Ahmed et al. [16] showed a thermal analysis of Maxwell nanofluid within the significance of H-SS. Xia et al. [17] highlighted physical significance of Eyring-Powell nanomaterial liquid flow with microorganisms and activation energy effects. Thumma et al. [18] explored the flow of nanofluid in the presence of a stretchable surface under the H-SS. Alharbi et al. [19] inspected the movement of nanoliquid on a flexible surface, emphasizing the importance of H-SS. Kumar et al. [20] explored the interaction between a dusty nanofluid stream past a gyrating disk in the presence of H-SS.

Due to its extensive industrial use, chemical reactions play a noteworthy role in heat and mass transfer research in scientific and engineering technology fields. Due to its vital role in the development of chemical processing equipment, the synthesis of polymers, cooling towers, pollution, the formation and dispersion of fog, temperature, and fiber insulation, among other things, it is determined to be necessary. Raw materials undergo chemical reactions in industrial chemical processes to convert basic raw resources into good products, such as oxidization and synthesis of components, food processing, moisture distribution in cultivated fields, crop damage due to cold, etc. Chemical variations of this kind are carried out inside a reactor. Kumar et al. [21] used a neural network scheme to elucidate the influence of chemical responses on liquid motion via a stretchy cylinder. Kodi and Mopuri [22] examined the flow of Casson liquid across an inclined permeable surface with the impact of a chemical reaction. Utilizing the numerical simulation, Karthik et al. [23] assessed the chemical reaction impact on the mass and heat transport study of the nanoliquid stream across an inclined cylinder. Saeed et al. [24] inspected the consequence of the chemical reaction of liquid flowing past a stretchable surface. Madhu et al. [25] assessed the consequence of chemical reaction on the liquid steam past a cylinder utilizing the collocation method.

In many engineering applications, the heat transfer analysis is improved by adding values resulting from the incorporation of thermal conductivity changes in heat transmission features. Examples of mixed conduction and radiation difficulties where temperature fluctuations and, therefore, thermal conductivity variations are noticeable include heat transfer in furnaces, fibrous and foam insulations, volumetric solar receivers, porous burners, and boilers. Srilatha et al. [26] probed the motion of nanofluid via a gyrating disk subjected to variable temperature conductivity. Fatima et al. [27] inspected the influence of nth-order chemical reaction on the three-dimensional viscoelastic nanofluids exposed to variable thermal conductivity. Mandal and Pal [28] analyzed the influence of thermal radiant energy on water hybrid nanoliquid flow past a permeable Riga surface. Additionally, the impact of variable temperature conductivity and variable viscosity were considered. The impact of activation energy, viscous dissipation, and variable thermal conductivity on the Eyring-Powell fluid flow via a porous medium was examined by Awais et al. [29]. Kodi et al. [30] studied the Maxwell nanofluid stream via a permeable medium past a perpendicular cone with heat conductivity and diffusion. Haq et al. [35] scrutinized thermal radiative heat flux impact in flow of viscous hybrid nanofluid by a porous moving cylinder. Kuang et al. [36] modeled and deliberated applications of thermodynamic extremal principle to diffusion controlled phase transformations. Devi and Prakash [37] and Khan et al. [38] recently explored characteristics of temperature dependent viscosity in stretchable flow of viscous and non-Newtonian fluid respectively. High performance MWC nano-polyvinylpyrrolidone/silicon based shear thickening material and experimental outcomes is explored by Sun et al. [39]. Mukhopadhyay and Layek [40] and Alhejaili et al. [41] discussed variable thermal conductivity effects in convective flow of viscous material flow towards a moving stretchable surface. Wang et al. [42] deliberated high speed photography and PIV (particle image velocimetry) methods to conduct experimental research into the fluid flow pattern and vortex field of cavitation in Venturi tubes. Miao and Massoudi [43] displayed the same behavior in flow of slag-type fluid with heat transport phenomenon. Fu et al. [44] displayed heat transport performance in aero-engine cooling using Wilson plot method of three analogous serpentine tube. Sulochana et al. [45] scrutinized influence of MWCNTs on hybrid bio-diesel blends for combustion in CI engines. Hou et al. [46] emphasized time dependent conjugate heat transport of heat wall for detonation combustor. Zhang et al. [47] worked on plug nozzle and Laval nozzle on the flow in the presence of non-premixed detonation combustor and the results of this research is published in Physics of Fluids.

The prime objective here is to analyze the radiating stagnation point stream of Maxwell nanomaterial by the stretched cylinder. Thermal and solutal convective conditions are discussed. The C-C heat flux model is used to discuss the mass and heat transport rate. Thermophoresis, chemical reaction, and random motion characteristics are deliberated. Additionally, heat generation and radiation are considered in energy expression. Nonlinear, non-dimensional ordinary systems are obtained through the implementation of adequate transformations. To construct convergent solutions, we implemented Homotopic analysis method [31-34]. Variations of temperature, liquid flow, and concentration against secondary variables are scrutinized via graphs.

International Journal of Engineering Research & Technology (IJERT)
ISSN: 2278-0181
Vol. 13 Issue 9, September 2024

2: MODELING

Consider steady flow of an incompressible stagnation point flow of Maxwell nanoliquid. The cylinder is stretched, having stretching velocity $\left(u = u_w = \frac{cx}{l}\right)$. The impact of Brownian diffusion, chemical reaction and thermophoresis features are considered. The C-C fluxes model is employed to discuss mass and heat transport rates. Effects of thermal radiation and heat generation are considered. The flow model schematic diagram is given in Fig. 1.

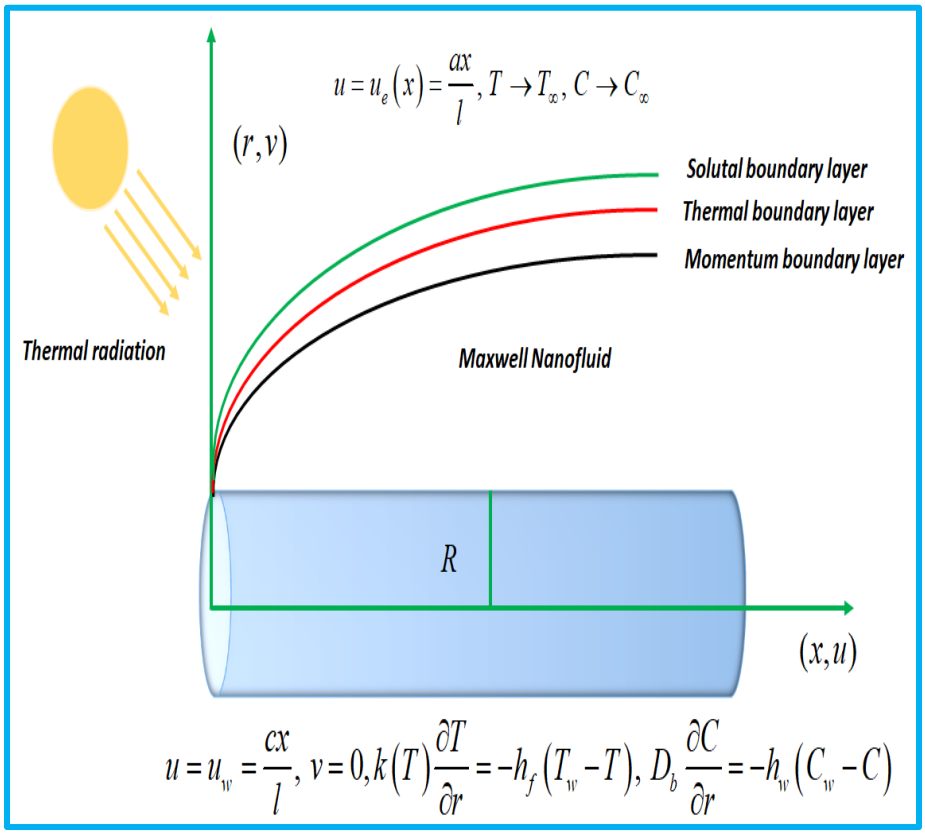

Fig. 1: Flow diagram.

The associated expressions under these assumptions are provided as follows.

$$\frac{\partial}{\partial x}(ru) + \frac{\partial}{\partial r}(rv) = 0, \tag{1}$$

$$u\frac{\partial u}{\partial x} + v\frac{\partial u}{\partial r} + \lambda_1\left(u^2\frac{\partial^2 u}{\partial x^2} + 2uv\frac{\partial^2 u}{\partial x \partial r} + v^2\frac{\partial^2 v}{\partial r^2}\right) = u_e\frac{\partial u_e}{\partial x} + \nu_f\left(\frac{1}{r}\frac{\partial u}{\partial r} + \frac{\partial^2 u}{\partial r^2}\right), \tag{2}$$

$$\left.\begin{aligned} u\frac{\partial T}{\partial x} + v\frac{\partial T}{\partial r} + \lambda_t\left(\begin{aligned} &u^2\frac{\partial^2 T}{\partial x^2} + u\frac{\partial u}{\partial x}\frac{\partial T}{\partial x} + u\frac{\partial v}{\partial x}\frac{\partial T}{\partial r} + 2uv\frac{\partial^2 T}{\partial x \partial r} + v\frac{\partial u}{\partial r}\frac{\partial T}{\partial x} \\ &+ v\frac{\partial v}{\partial r}\frac{\partial T}{\partial r} + v^2\frac{\partial^2 T}{\partial r^2}\end{aligned}\right) \\ = \frac{k(T)}{(\rho c_p)_f}\left(1 + \frac{16\sigma^* T_\infty^3}{3k_f k^*}\right)\left(\frac{1}{r}\frac{\partial T}{\partial r} + \frac{\partial^2 T}{\partial r^2}\right) + \tau\left(D_b\frac{\partial T}{\partial r}\frac{\partial C}{\partial r} + \frac{D_t}{T_\infty}\left(\frac{\partial T}{\partial r}\right)^2\right) + \frac{Q_0}{(\rho c_p)_f}(T - T_\infty)\end{aligned}\right\}, \tag{3}$$

International Journal of Engineering Research & Technology (IJERT)
ISSN: 2278-0181
Vol. 13 Issue 9, September 2024

$$\left.\begin{aligned} u\frac{\partial C}{\partial x}+v\frac{\partial C}{\partial r}+\lambda_c\left(\begin{aligned} &u^2\frac{\partial^2 C}{\partial x^2}+u\frac{\partial u}{\partial x}\frac{\partial C}{\partial x}+u\frac{\partial v}{\partial x}\frac{\partial C}{\partial r}+2uv\frac{\partial^2 C}{\partial x\partial r}\\ &+v\frac{\partial u}{\partial r}\frac{\partial C}{\partial x}+v\frac{\partial v}{\partial r}\frac{\partial C}{\partial r}+v^2\frac{\partial^2 C}{\partial r^2}\end{aligned}\right)\\ =D_b\left(\frac{1}{r}\frac{\partial C}{\partial r}+\frac{\partial^2 C}{\partial r^2}\right)+\frac{D_t}{T_\infty}\left(\frac{1}{r}\frac{\partial T}{\partial r}+\frac{\partial^2 T}{\partial r^2}\right)-k_r(C-C_\infty)\end{aligned}\right\}, \tag{4}$$

with

$$\left.\begin{aligned} u=u_w(x)=\tfrac{cx}{l},\ \ v=0,\ \ k(T)\tfrac{\partial T}{\partial r}=-h_f(T_w-T),\ D_b\tfrac{\partial C}{\partial r}=-h_w(C_w-C)\ \text{at } r=R\\ u=u_e(x)=\tfrac{ax}{l},\quad T\to T_\infty, C\to C_\infty\ \ \text{as } r\to\infty\end{aligned}\right\}. \tag{5}$$

Let the transformations

$$\left.\begin{aligned} u=\tfrac{cx}{l}f'(\eta),\ \ v=-\tfrac{R}{r}\sqrt{\tfrac{c\nu_f}{l}}f(\eta),\ \ \theta(\xi,\eta)=\tfrac{T-T_\infty}{T_w-T_\infty}\\ \phi(\xi,\eta)=\tfrac{C-C_\infty}{C_w-C_\infty},\ \eta=\sqrt{\tfrac{c}{\nu_f l}}\left(\tfrac{r^2-R^2}{2R}\right)\end{aligned}\right\}, \tag{6}$$

$$(1+2\omega\eta)f'''+2\omega f''-f'^2+ff''+\alpha_1\left(-f^2f'''-\frac{\omega}{(1+2\omega\eta)}f^2f''+2ffff''\right)+A^2=0, \tag{7}$$

$$\left.\begin{aligned} (1+\in\theta+Rd)\left((1+2\omega\eta)\theta''+2\omega\theta'\right)+\in(1+2\omega\eta)\theta'^2+\Pr f\theta'+\Pr Q\theta-\Pr\alpha_t\left(f^2\theta''+ff'\theta'\right)\\ +\Pr(1+2\omega\eta)\left(Nt\theta'^2+Nb\theta'\phi'\right)=0\end{aligned}\right\}, \tag{8}$$

$$\left.\begin{aligned} (1+2\omega\eta)\phi''+2\omega\phi'+Scf\phi'-Sc\alpha_c\left(f^2\phi''+ff'\phi'\right)\\ +\tfrac{Nt}{Nb}\left((1+2\omega\eta)\theta''+2\omega\theta'\right)-Sc\gamma\phi=0\end{aligned}\right\}, \tag{9}$$

with

$$\left.\begin{aligned} f'(0)=1,\ f(0)=0,\ \ (1+\in\theta(0))\theta'(0)=-\gamma_1(1-\theta(0))\\ \phi'(0)=-\gamma_2(1-\phi(0)),\ f'(\infty)=A,\ \ \theta(\infty)=0,\ \ \phi(\infty)=0\end{aligned}\right\}. \tag{10}$$

With the variable thermal conductivity

$$k(T)=k_f\left(1+\in\left(\frac{T-T_\infty}{T_w-T_\infty}\right)\right) \tag{11}$$

Here the dimensionless variables are $\omega\left(=\sqrt{\frac{\nu_f l}{cR^2}}\right)$, $\Pr\left(=\frac{\nu_f}{\alpha^*}\right)$, $\alpha_1\left(=\frac{\lambda_1 c}{l}\right)$, $Rd\left(=\frac{16\sigma^* T_\infty^3}{3k^* k_f}\right)$, $\gamma\left(=\frac{k_r l}{c}\right)$, $Q\left(=\frac{Q_0 l}{c(\rho c_p)_f}\right)$, $\alpha_t\left(=\lambda_t\frac{c}{l}\right)$, $\alpha_c\left(=\lambda_c\frac{c}{l}\right)$, $Sc\left(=\frac{\nu_f}{D_b}\right)$, $Nt\left(=\frac{\tau D_t(T_w-T_\infty)}{\nu_f T_\infty}\right)$, $Nb\left(=\frac{\tau D_b(C_w-C_\infty)}{\nu_f}\right)$, $\gamma_1\left(=\frac{h_f}{k_f}\sqrt{\frac{\nu_f l}{c}}\right)$, $\gamma_2\left(=\frac{h_w}{D_b}\sqrt{\frac{\nu_f l}{c}}\right)$ and $A\left(=\frac{a}{c}\right)$.

International Journal of Engineering Research & Technology (IJERT)
ISSN: 2278-0181
Vol. 13 Issue 9, September 2024

3: PHYSICAL QUANTITIES

3.1: Nusselt number

We can express that

$$Nu_x = \frac{xq_w}{k_f\left(T_w - T_\infty\right)}, \tag{12}$$

in which heat flux q_w is

$$q_w = -\left(k\left(T\right) + \frac{16\sigma^* T_\infty^3}{3k^*}\right)\left(\frac{\partial T}{\partial r}\right)\Bigg|_{r=R}. \tag{13}$$

Dimensionless version is

$$Nu_x \,\mathrm{Re}_x^{-1/2} = -\left(1 + \in \theta\left(0\right) + Rd\right)\theta'\left(0\right). \tag{14}$$

3.2: Sherwood number

It is expressed as

$$Sh_x = \frac{xj_w}{D_B\left(C_w - C_\infty\right)}, \tag{15}$$

in which j_w mass flux obeys

$$j_w = -D_B\left(\frac{\partial C}{\partial r}\right)\Bigg|_{r=R}. \tag{16}$$

Finally, we get

$$Sh_x \,\mathrm{Re}_x^{-1/2} = -\phi'\left(0\right). \tag{17}$$

4: SOLUTION METHODOLOGY

Here, we used the Homotopy analysis method (HAM) to get the convergent series solutions for nonlinear, non-dimensional ordinary expressions [31-34]. This approach needs early guesses and linear operators well-defined below.

$$\left.\begin{aligned} f_0\left(\eta\right) &= 1 - e^{-\eta} \\ \theta_0\left(\eta\right) &= \tfrac{\gamma_1}{1+\gamma_1} e^{-\eta} \\ \phi_0\left(\eta\right) &= \tfrac{\gamma_2}{1+\gamma_2} e^{-\eta} \end{aligned}\right\}, \tag{18}$$

$$\left.\begin{aligned} L_f &= \tfrac{\partial^3}{\partial\eta^3} - \tfrac{\partial}{\partial\eta} \\ L_\theta &= \tfrac{\partial^2}{\partial\eta^2} - 1 \\ L_\phi &= \tfrac{\partial^2}{\partial\eta^2} - 1 \end{aligned}\right\}, \tag{19}$$

with

$$\left.\begin{aligned} L_f[b_0 + b_1 e^{-\eta} + b_2 e^{\eta}] = 0,\;\; L_\theta[b_3 e^{-\eta} + b_4 e^{\eta}] = 0, \\ L_\phi[b_5 e^{-\eta} + b_6 e^{\eta}] = 0. \end{aligned}\right\}. \tag{20}$$

Here $b_i\left(i = 0,\ 1,\ 2,...,6\right)$ indicate the arbitrary quantities.

Published by :
http://www.ijert.org

International Journal of Engineering Research & Technology (IJERT)
ISSN: 2278-0181
Vol. 13 Issue 9, September 2024

5: SOLUTIONS CONVERGENCE

In homotopic technique the key parameters responsible for solutions convergence are ($\hbar_f$, $\hbar_\theta$, $\hbar_\phi$). For acceptable regions of these variables $\hbar-$ curves have been sketched in Fig. 2. The range for meaningful standards are $-1.5 \le \hbar_f \le -0.4$, $-1.7 \le \hbar_f \le -0.2$ and $-1.6 \le \hbar_f \le -0.3$.

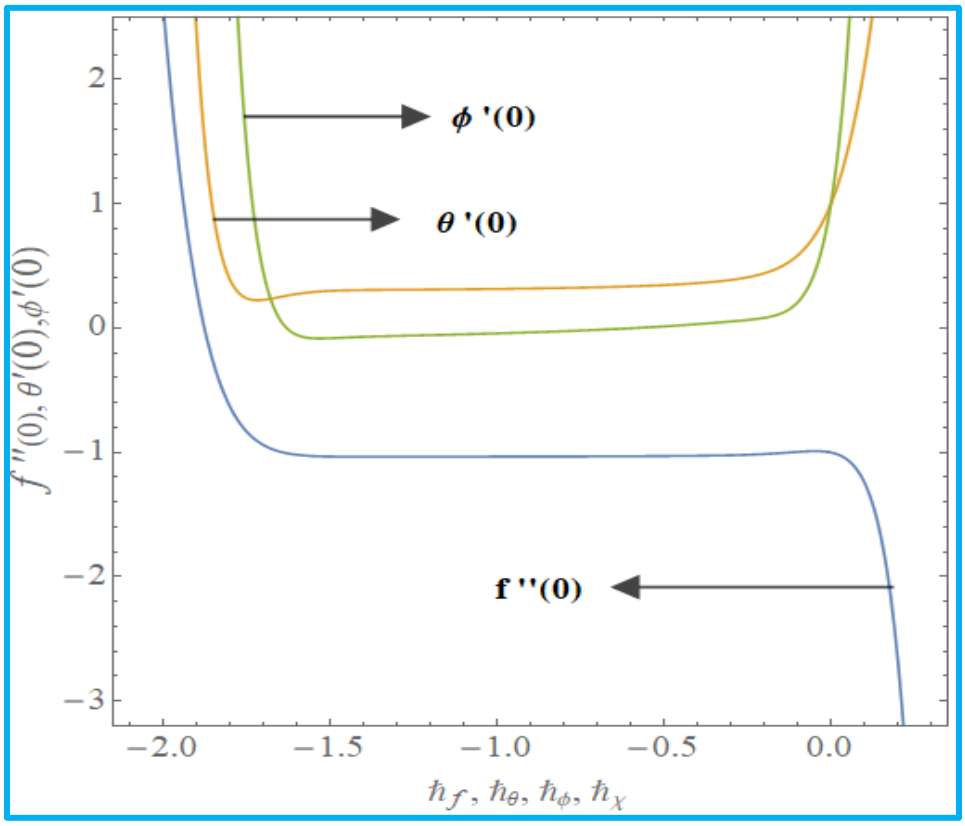

Fig. 2: combine $\hbar$-curves.

6: RESULTS AND DISCUSSION

It is discussed how different metrics on physical measurements may be physically clarified.

6.1: VELOCITY

Fig. 3 is sketched to show the examine the variation of curvature variable (ω) against velocity ($f'(\eta)$). Clearly velocity increase for higher value of curvature variable. Variation of (A) on velocity is revealed in Fig. 4. For higher estimation of stretching ratio variable fluid flow enhances. However, boundary layer thickness has contradictory features for $A>1$ and $A<1$. For $A=1$ there is no boundary layer formation. Fig. 5 disclosed the characteristics of Maxwell fluid parameter (α_1) on velocity field. Here fluid flow declined against fluid parameter.

Published by :
http://www.ijert.org

International Journal of Engineering Research & Technology (IJERT)
ISSN: 2278-0181
Vol. 13 Issue 9, September 2024

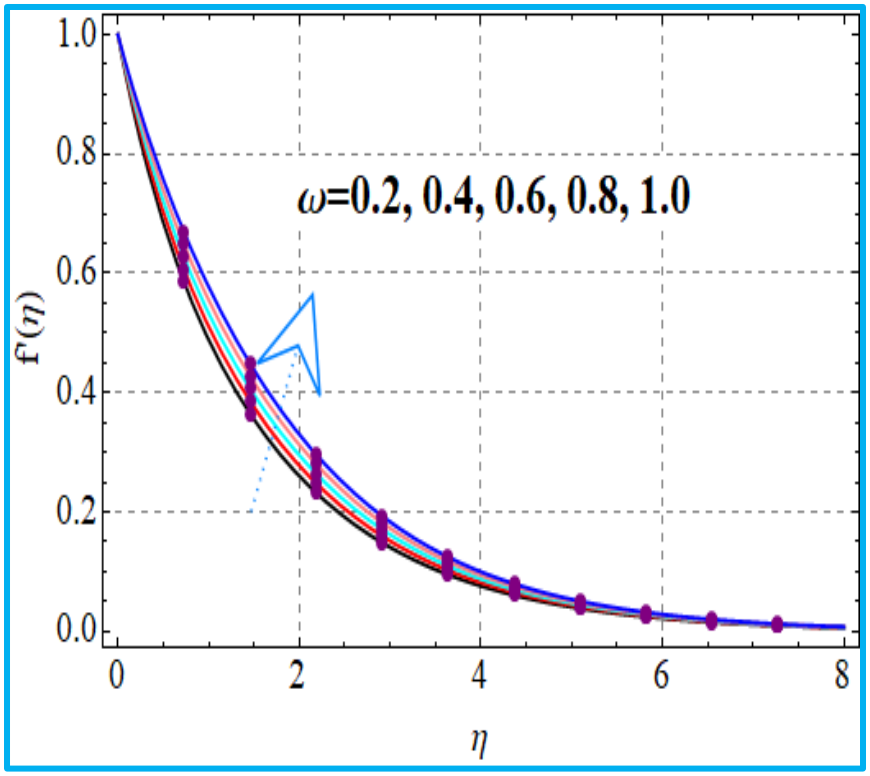

Fig. 3: $f'(\eta)$ vs ω.

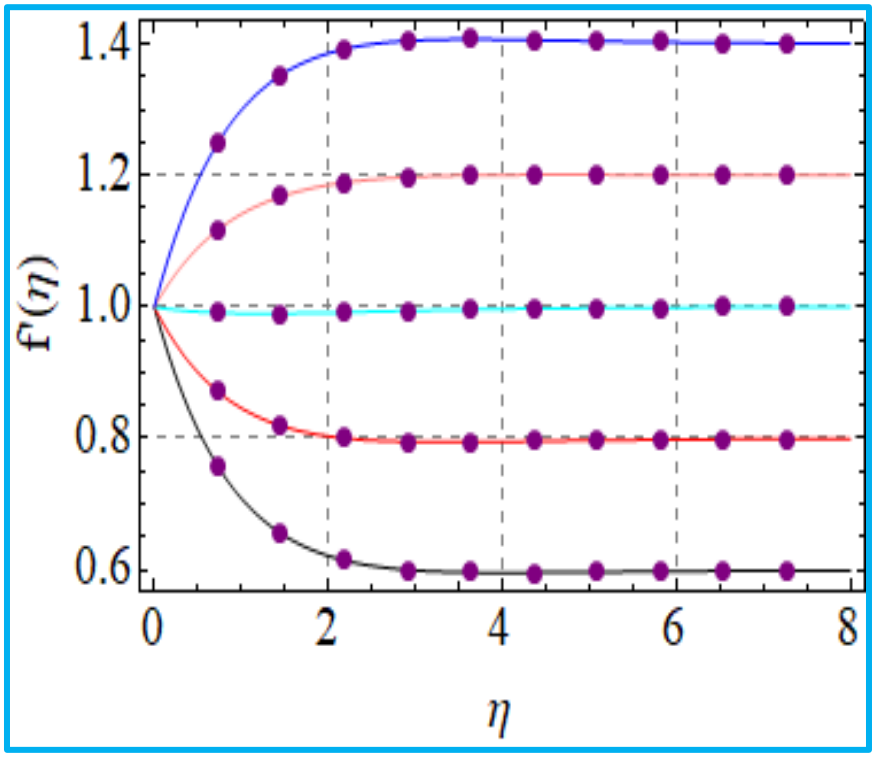

Fig. 4: $f'(\eta)$ vs A.

International Journal of Engineering Research & Technology (IJERT)
ISSN: 2278-0181
Vol. 13 Issue 9, September 2024

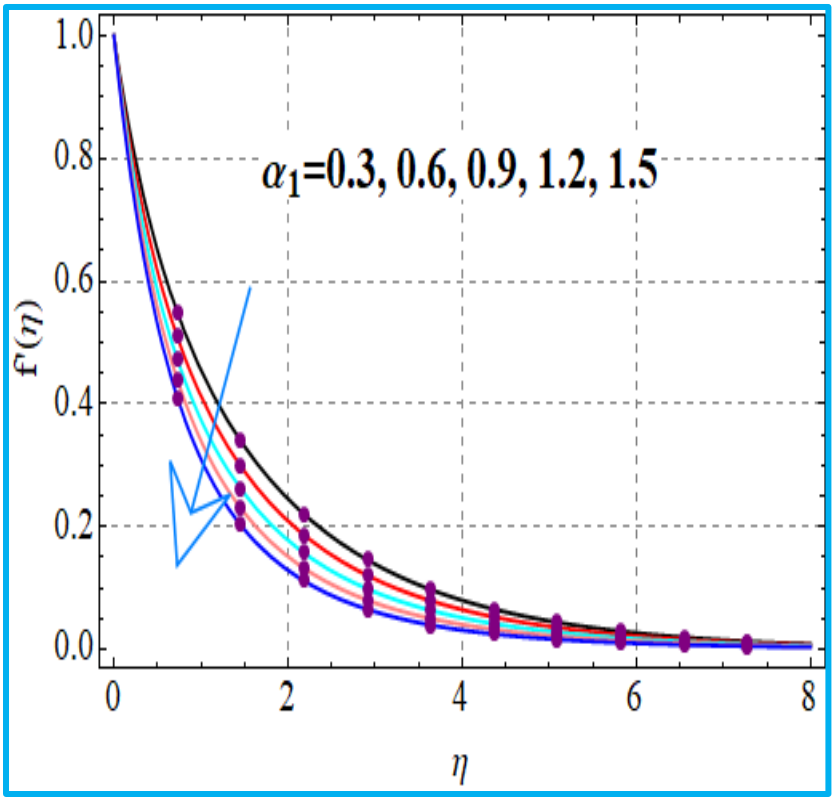

Fig. 5: $f'(\eta)$ vs α_1.

6.2: Temperature

The effect of γ_1 on $\theta(\eta)$ is sketched in Fig. 6. Thermal field has increasing behavior for higher values of thermal Biot number. Figs. (7 and 8) show the behavior of variable thermal conductivity ($\in$) and thermal relaxation time (α_t) parameters on the thermal field. The increment is observed in thermal distribution for higher estimation of ($\in$) and (α_t). The influence of thermophoresis and random motion variables on temperature is depicted in Figs. (9 and 10). Fig. 9 exhibits that for higher values of thermophoresis variable (Nt) temperature enhances. Fig. 10 shows that a larger random motion variable (Nb) enhances the collision between nanoparticles and, as a result, thermal distribution upsurges. Fig 9 shows the impact of Nt on $\theta(\eta)$ for two different flow cases. The rise in values of Nt improves the $\theta(\eta)$ for both flow cases. As a result of thermophoresis, which moves nanoparticles from hot to cold areas, the thermal profile rises with the thermophoresis parameter values. By improving heat transport within the fluid, this movement helps to more evenly distribute thermal energy. There is an elevated thermal profile throughout the fluid as a result of nanoparticles' ability to transfer heat from hotter regions to cooler ones. Fig 10 displays the impact of Nb on $\theta(\eta)$ for two different flow cases. The escalation in values of Nb advances the $\theta(\eta)$ for both flow cases. Since increased Brownian motion causes more intense and frequent collisions between nanoparticles. More heat transport and energy exchange within the fluid are made possible by these encounters. Consequently, the fluid's total temperature rises due to the higher thermal conductivity brought on by greater Brownian motion, raising the thermal profile. Fig. 11 demonstrates the effect of the heat generation variable (Q) on temperature. Larger (Q) produced more heat in the system which give rise to the temperature of the fluid.

Published by :
http://www.ijert.org

International Journal of Engineering Research & Technology (IJERT)
ISSN: 2278-0181
Vol. 13 Issue 9, September 2024

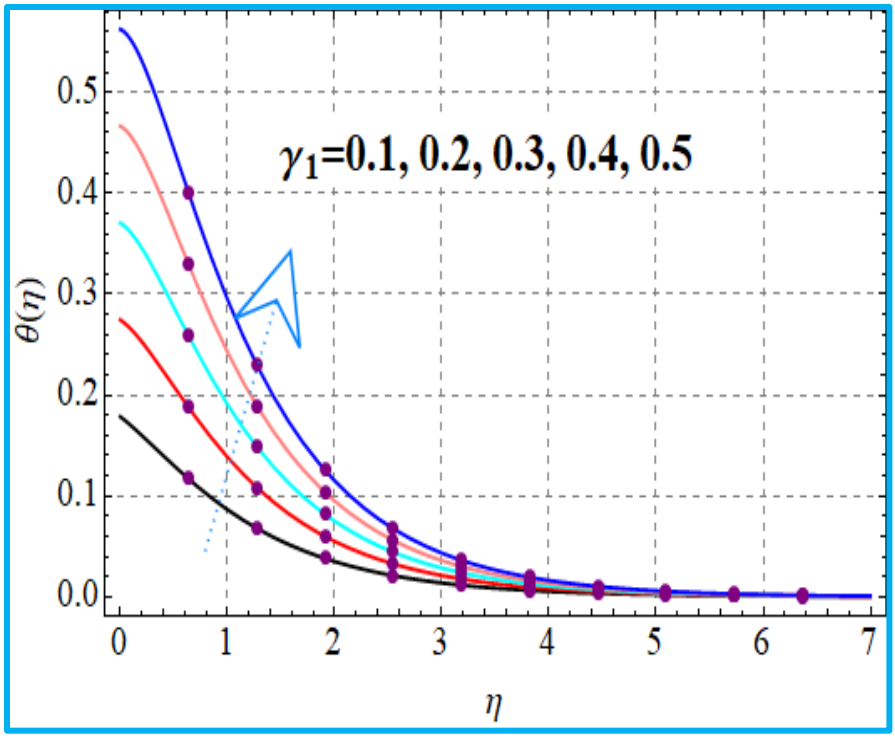

Fig. 6: vs γ_1.

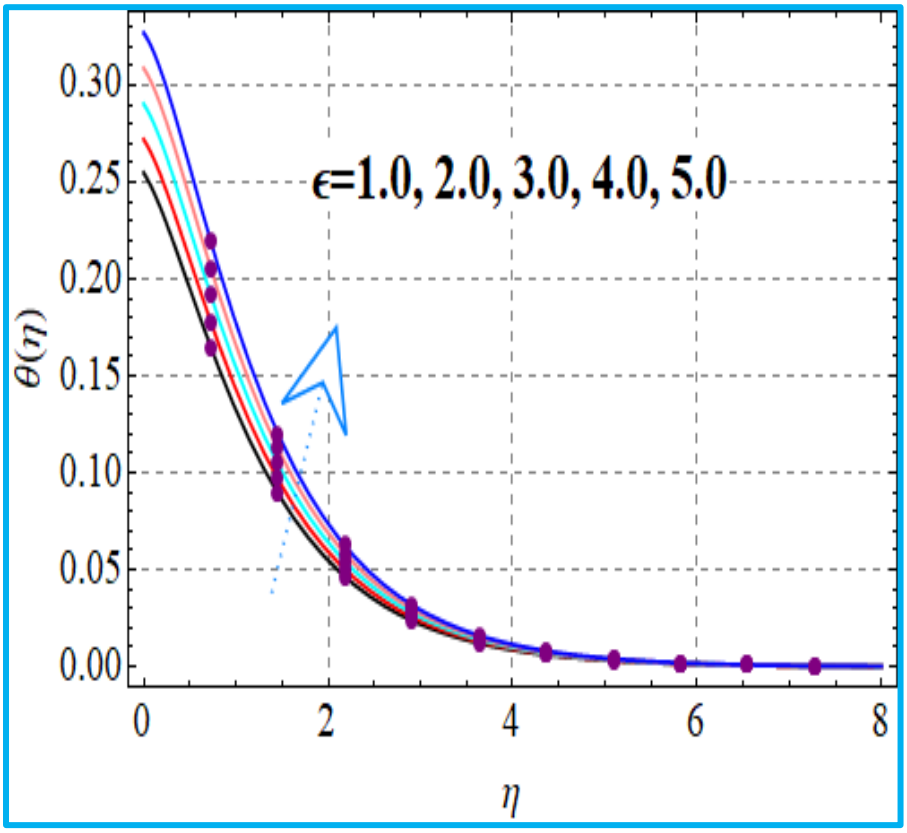

Fig. 7: vs $\in$.

Published by :
http://www.ijert.org

International Journal of Engineering Research & Technology (IJERT)
ISSN: 2278-0181
Vol. 13 Issue 9, September 2024

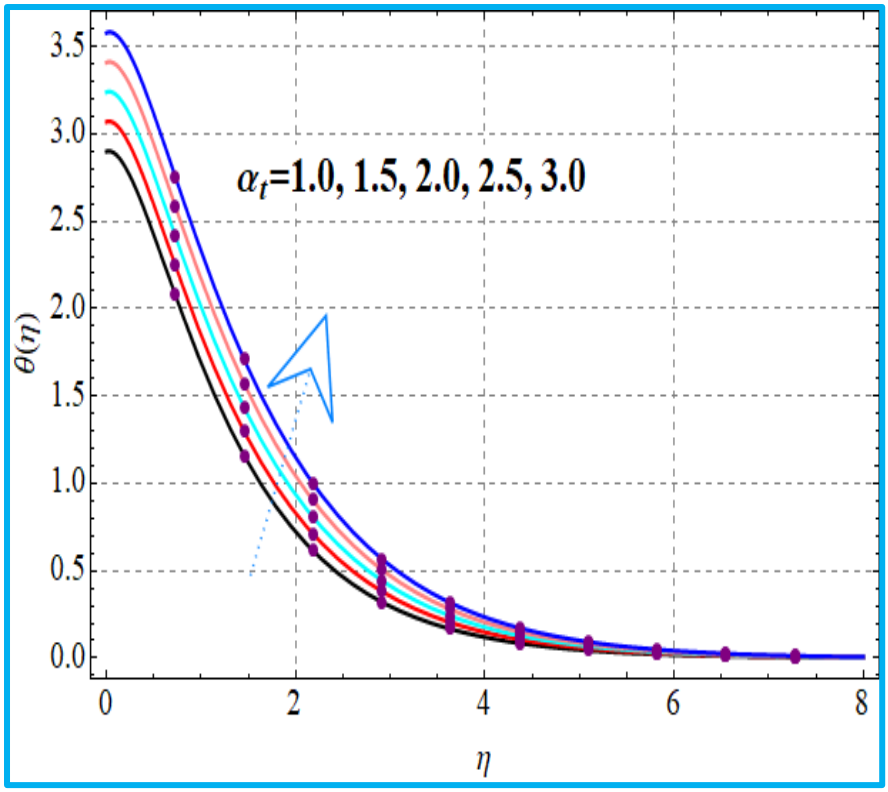

Fig. 8: vs α_t.

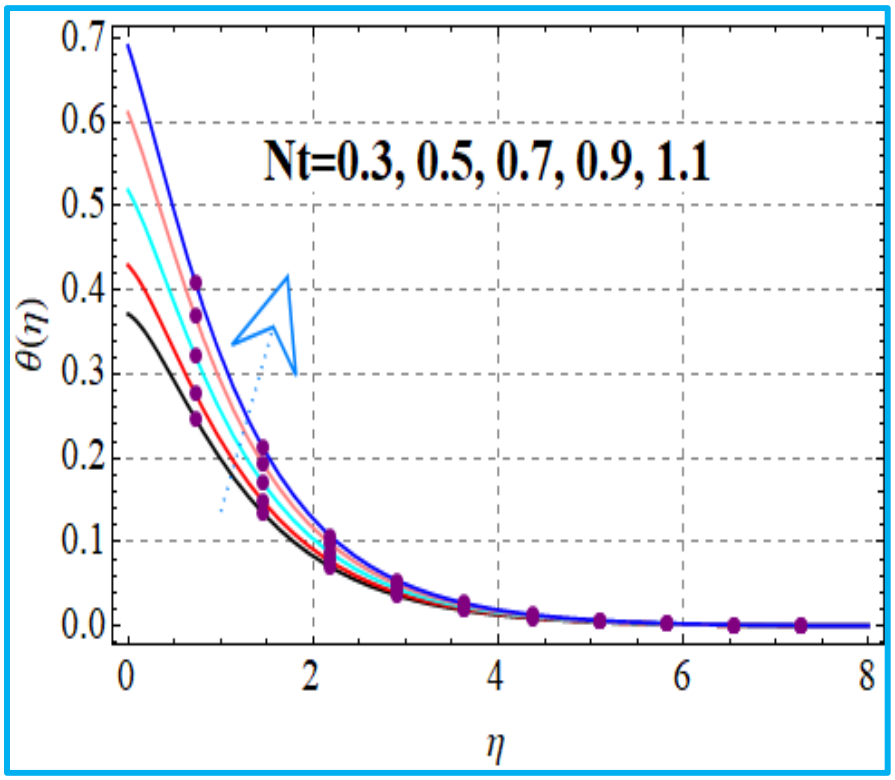

Fig. 9: $\theta(\eta)$ vs Nt.

Published by :
http://www.ijert.org

International Journal of Engineering Research & Technology (IJERT)
ISSN: 2278-0181
Vol. 13 Issue 9, September 2024

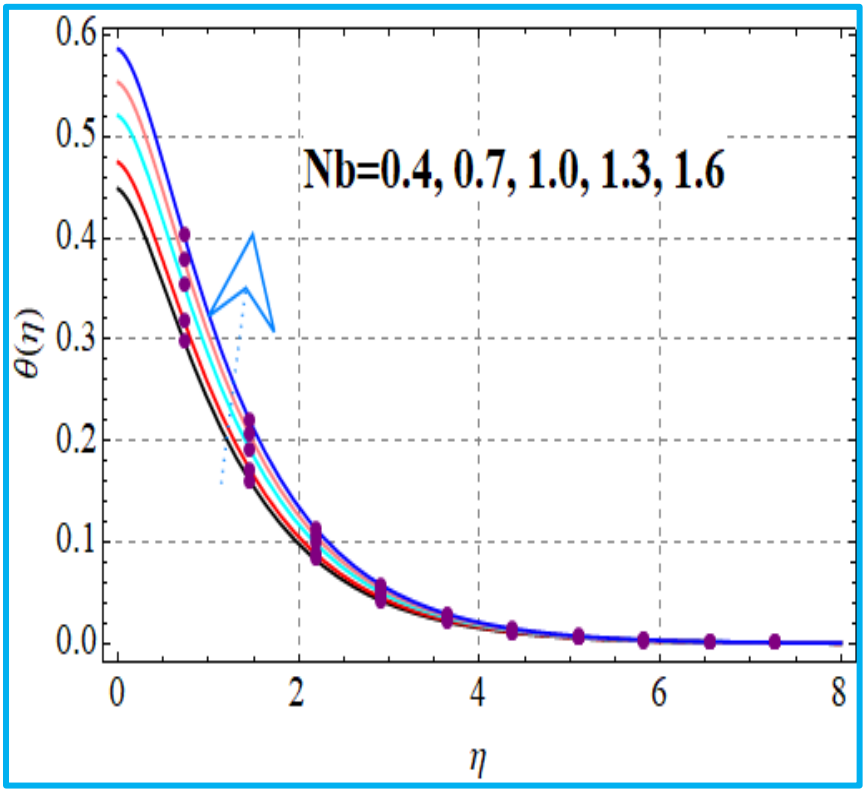

Fig. 10: vs Nb.

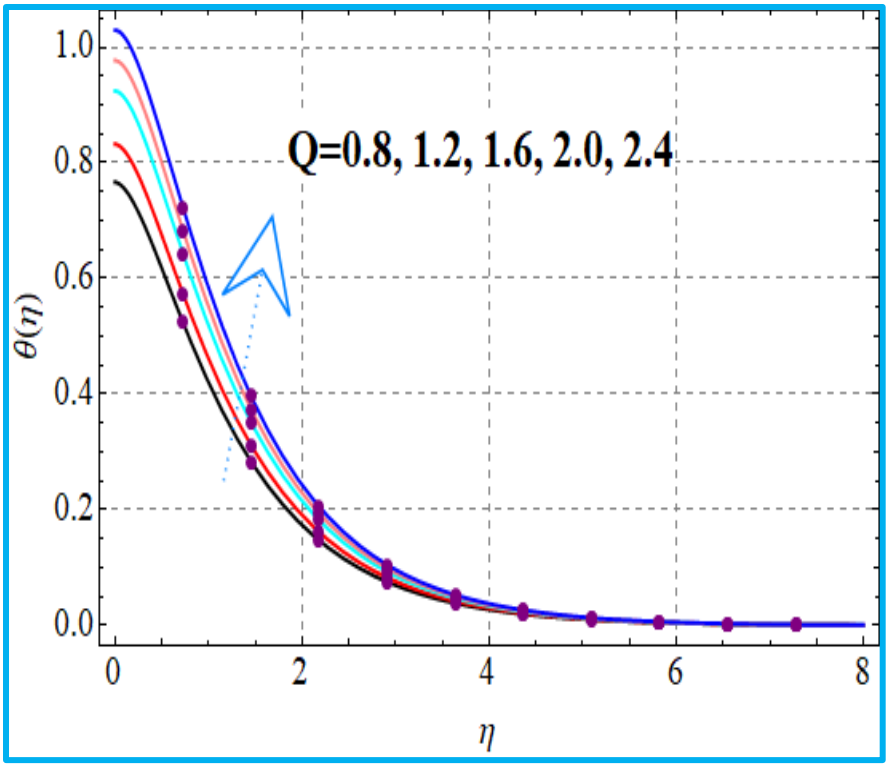

Fig. 11: vs Q.

International Journal of Engineering Research & Technology (IJERT)
ISSN: 2278-0181
Vol. 13 Issue 9, September 2024

6.3: Concentration

The effect of α_c on concentration is explored in Fig. 12. Higher α_c improves the fluid $\phi(\eta)$. Fig. 13 displays the outcome of concentration for the solutal Biot number (γ_2). It is witnessing that concentration increases for higher solutal Biot numbers. Fig. 14 represents the impact of the γ on concentration. A decrement in concentration is observed for larger (γ).Fig 15 displays the influence of Nt on $\phi(\eta)$. Here, the rise in values of Nt increases the $\phi(\eta)$. Because of the migration of nanoparticles from high-temperature areas to low-temperature regions brought on by thermophoresis. This movement increases the local concentration of nanoparticles by concentrating them in colder areas. A greater concentration profile is produced throughout the fluid as a consequence of the concentration gradient being steeper. As a result, thermophoresis improves nanoparticle localization and increases concentration in regions that are affected by temperature gradients. The Influence of Nb on $\phi(\eta)$ is displayed in Fig 16. Here, the rise in values of Nb decreases the $\phi(\eta)$. Because higher Brownian motion causes more random movement of particles within the fluid. Because of this improved mobility, nanoparticles are distributed more evenly throughout the fluid, which lowers local concentrations close to the surface or source. Particle distribution becomes more uniform as a consequence, which lowers the concentration gradient and the fluid's overall concentration profile.

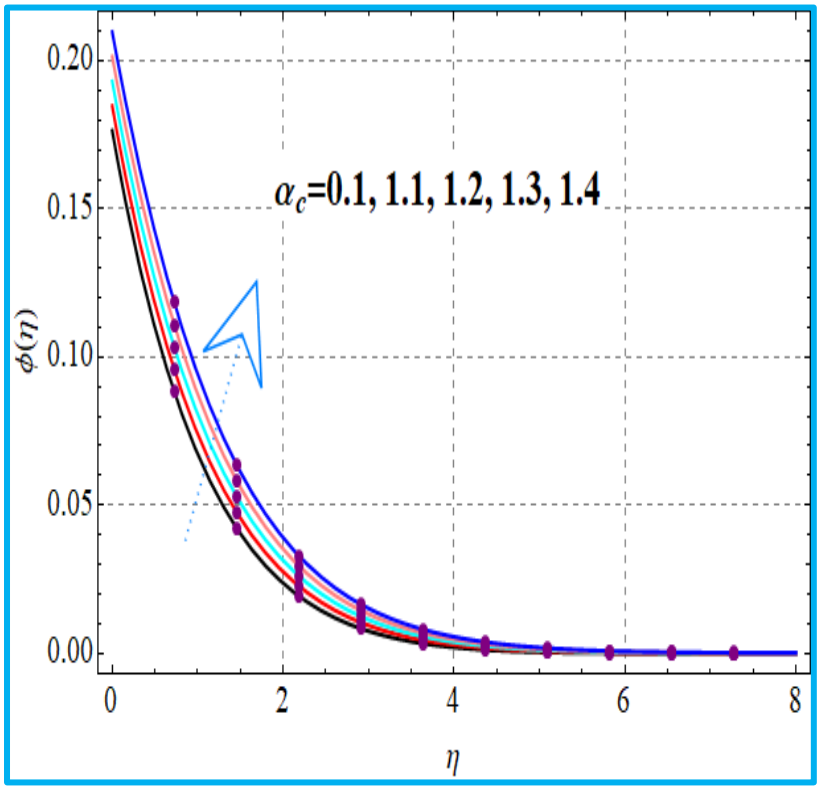

Fig. 12: $\phi(\eta)$ vs α_c.

Published by :
http://www.ijert.org

International Journal of Engineering Research & Technology (IJERT)
ISSN: 2278-0181
Vol. 13 Issue 9, September 2024

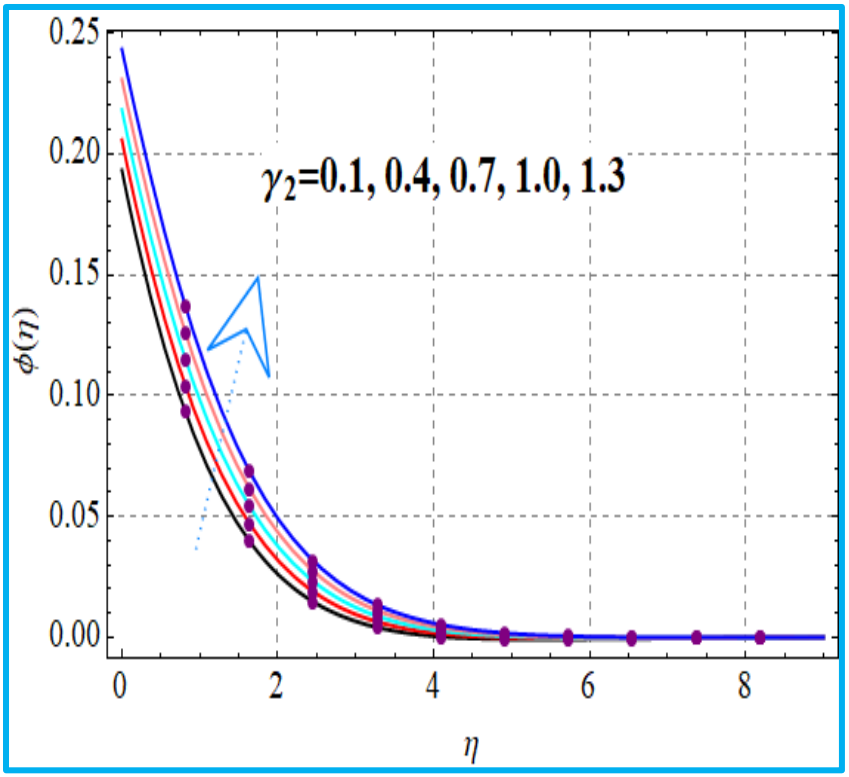

Fig. 13: $\phi(\eta)$ vs λ_2.

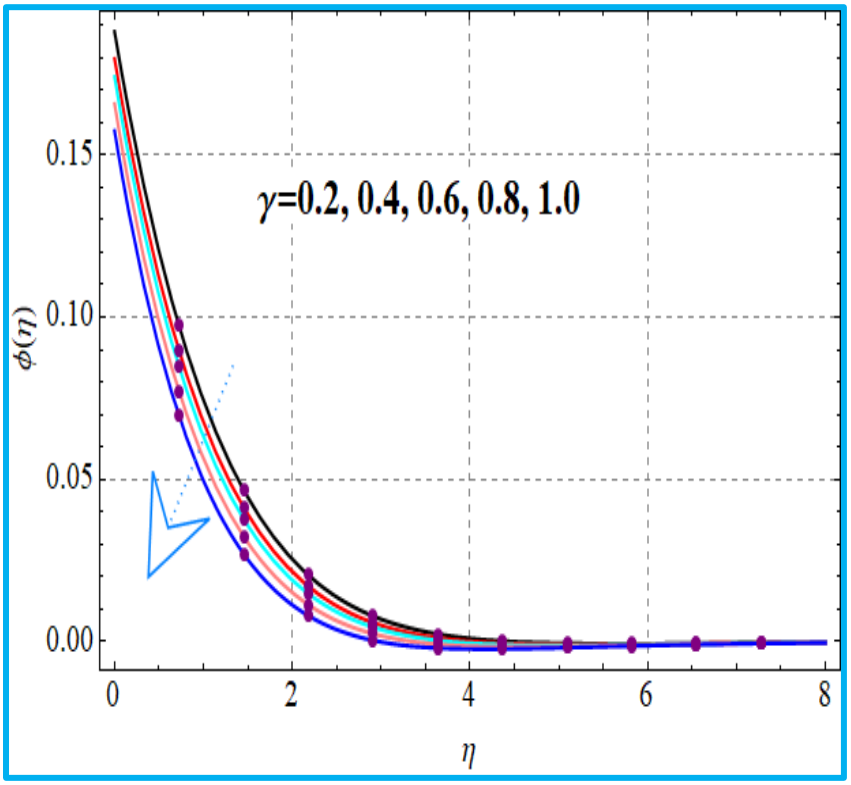

Fig. 14: $\phi(\eta)$ vs γ.

International Journal of Engineering Research & Technology (IJERT)
ISSN: 2278-0181
Vol. 13 Issue 9, September 2024

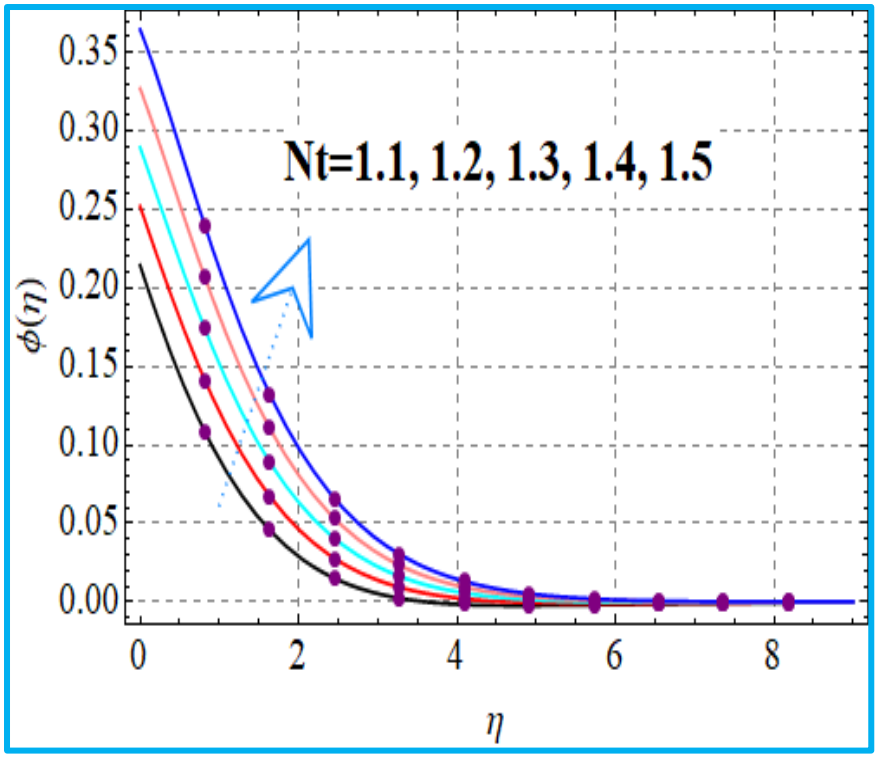

Fig. 15: $\phi(\eta)$ vs Nt.

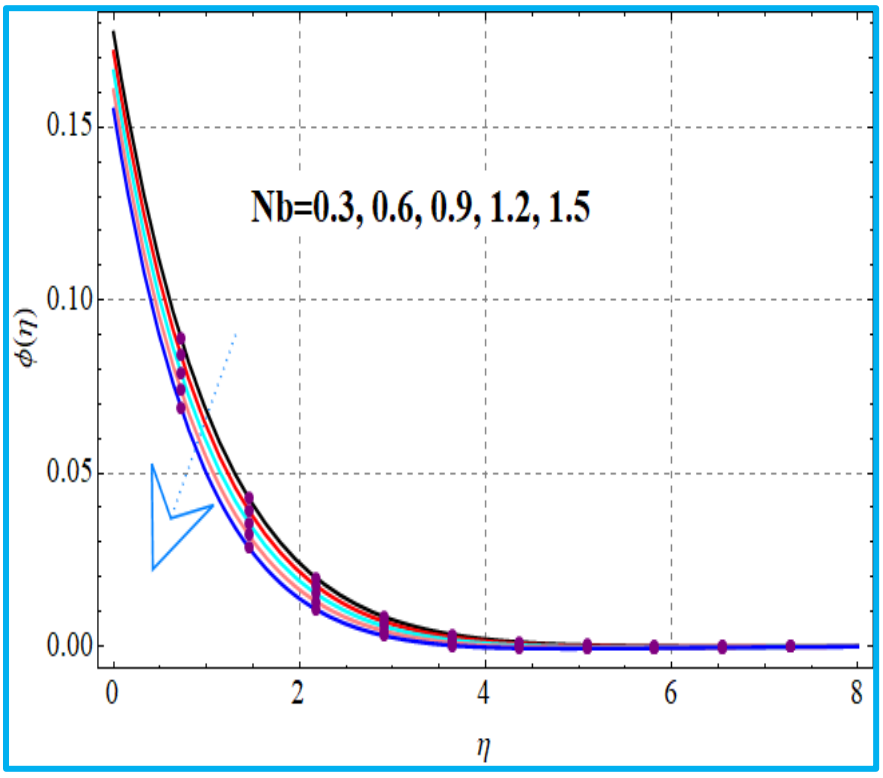

Fig. 16: $\phi(\eta)$ vs Nb.

International Journal of Engineering Research & Technology (IJERT)
ISSN: 2278-0181
Vol. 13 Issue 9, September 2024

7: CLOSING REMARKS

The consequence of heat source and chemical reactions on the stream of Maxwell liquid via a stretching cylinder with variable thermal conductivity and radiation is analyzed in the current study. It is expected that the flow is produced by the stretchy effect of the cylinder. The C-C heat flux model is applied to study the heat and mass transport attributes of the fluid flow. The governing equations of the study are transformed into ODEs employing similarity variables. Additionally, the resultant ODEs are solved utilizing the HAM scheme. The graphical depiction shows the impact of several constraints on the various profiles. The key observations from the above analysis are,

- Higher material variable corresponds to declines in liquid flow.
- An upsurge in curvature variable results in velocity enhancement.
- An intensification in thermal distribution for thermal conductivity variable.
- Temperature augmentation for higher thermal relaxation variables is noticed.
- Higher heat generation variable boosts thermal distribution.
- Higher thermal and solutal Biot numbers lead to a rise in concentration and thermal distribution.
- Reduction in concentration occurs for higher random motion and reaction variables.
- Higher solutal relaxation variable augments concentration, and a similar impact was noticed for the thermophoresis variable.
- An increment in thermal distribution for higher Brownian motion and thermophoresis parameters is witnessed.

DECLARATIONS

Ethics approval and consent to participate: Not applicable
Consent for publication: Not applicable
Availability of data and materials: All data used in this manuscript have been presented within the article.
Competing Interests: The authors declare that they have no competing interests.
Acknowledgments: Researchers Supporting Project number (RSPD2024R576), King Saud University, Riyadh, Saudi Arabia.
Authors' contributions: All authors are equally contributed in the research work.

REFERENCES

[1] A. M. Megahed, “Improvement of heat transfer mechanism through a Maxwell fluid flow over a stretching sheet embedded in a porous medium and convectively heated,” Mathematics and Computers in Simulation, vol. 187, pp. 97–109, Sep. 2021, doi: 10.1016/j.matcom.2021.02.018.
[2] J. O. Olabode, A. S. Idowu, M. T. Akolade, and E. O. Titiloye, “Unsteady flow analysis of Maxwell fluid with temperature dependent variable properties and quadratic thermo-solutal convection influence,” Partial Differential Equations in Applied Mathematics, vol. 4, p. 100078, Dec. 2021, doi: 10.1016/j.padiff.2021.100078.
[3] V. Kumar, J. K. Madhukesh, A. M. Jyothi, B. C. Prasannakumara, M.I. Khan, and Y. M. Chu, "Analysis of single and multi-wall carbon nanotubes (SWCNT/MWCNT) in the flow of Maxwell nanofluid with the impact of magnetic dipole," Computational and Theoretical Chemistry, vol. 1200, Article No. 113223, June 2021, https://doi.org/10.1016/j.comptc.2021.113223.
[4] I. Khan, A. Raza, M. A. Shakir, A. S. Al-Johani, A. A. Pasha, and K. Irshad, “Natural convection simulation of Prabhakar-like fractional Maxwell fluid flowing on inclined plane with generalized thermal flux,” Case Studies in Thermal Engineering, vol. 35, p. 102042, Jul. 2022, doi: 10.1016/j.csite.2022.102042.
[5] T. Salahuddin, Z. Mahmood, M. Khan, and M. Awais, “A permeable squeezed flow analysis of Maxwell fluid near a sensor surface with radiation and chemical reaction,” Chemical Physics, vol. 562, p. 111627, Oct. 2022, doi: 10.1016/j.chemphys.2022.111627.
[6] C. Kumar et al., “A physics-informed machine learning prediction for thermal analysis in a convective-radiative concave fin with periodic boundary conditions,” ZAMM - Journal of Applied Mathematics and Mechanics / Zeitschrift für Angewandte Mathematik und Mechanik, vol. 104, no. 7, p. e202300712, 2024, doi: 10.1002/zamm.202300712.
[7] M. A. Kumar, Y. D. Reddy, V. S. Rao, and B. S. Goud, “Thermal radiation impact on MHD heat transfer natural convective nano fluid flow over an impulsively started vertical plate,” Case Studies in Thermal Engineering, vol. 24, p. 100826, Apr. 2021, doi: 10.1016/j.csite.2020.100826.
[8] D. Yu and R. Wang, “An Optimal Investigation of Convective Fluid Flow Suspended by Carbon Nanotubes and Thermal Radiation Impact,” Mathematics, vol. 10, no. 9, Art. no. 9, Jan. 2022, doi: 10.3390/math10091542.
[9] Y. J. Lim, Sharidan Shafie, Sharena Mohamad Isa, N. A. Rawi, and A. Q. Mohamad, “Impact of chemical reaction, thermal radiation and porosity on free convection Carreau fluid flow towards a stretching cylinder,” Alexandria Engineering Journal, vol. 61, no. 6, pp. 4701–4717, Jun. 2022, doi: 10.1016/j.aej.2021.10.023.
[10] K. S. Albalawi et al., “Nanoparticle aggregation kinematics and nanofluid flow in convectively heated outer stationary and inner stretched coaxial cylinders: Influenced by linear, nonlinear, and quadratic thermal radiation,” Mod. Phys. Lett. B, p. 2450361, May 2024, doi: 10.1142/S0217984924503615.
[11] R. J. Punith Gowda, R. Naveen Kumar, R. Kumar, and B. C. Prasannakumara, “Three-dimensional coupled flow and heat transfer in non-newtonian magnetic nanofluid: An application of Cattaneo-Christov heat flux model,” Journal of Magnetism and Magnetic Materials, vol. 567, p. 170329, Feb. 2023, doi: 10.1016/j.jmmm.2022.170329.

[12]R. J. P. Gowda, R. N. Kumar, A. Rauf, B. C. Prasannakumara, and S. A. Shehzad, “Magnetized flow of sutterby nanofluid through cattaneo-christov theory of heat diffusion and stefan blowing condition,” Appl Nanosci, vol. 13, no. 1, pp. 585–594, Jan. 2023, doi: 10.1007/s13204-021-01863-y.
[13]M. Jawad and K. S. Nisar, “Upper-convected flow of Maxwell fluid near stagnation point through porous surface using Cattaneo-Christov heat flux model,” Case Studies in Thermal Engineering, vol. 48, p. 103155, Aug. 2023, doi: 10.1016/j.csite.2023.103155.
[14]A. Hussain and Z. Mao, “Heat transfer analysis of MHD Prandtl-Eyring fluid flow with Christov-Cattaneo heat flux model,” Numerical Heat Transfer, Part A: Applications, vol. 0, no. 0, pp. 1–21, doi: 10.1080/10407782.2024.2316208.
[15]Y. X. Li, K. Al-Khaled, S. U. Khan, T. C. Sun, M. I. Khan, and M. Y. Malik, "Bio-convective Darcy-Forchheimer periodically accelerated flow of non-Newtonian nanofluid with Cattaneo-Christov and Prandtl effective approach," Case Studies in Thermal Engineering, vol. 26, Article No. 101102, Aug. 2021, https://doi.org/10.1016/j.csite.2021.101102.
[16]A. Ahmed, M. Khan, A. Hafeez, and J. Ahmed, “Thermal analysis in unsteady radiative Maxwell nanofluid flow subject to heat source/sink,” Appl Nanosci, vol. 10, no. 12, pp. 5489–5497, Dec. 2020, doi: 10.1007/s13204-020-01431-w.
[17]W. F. Xia, F. Haq, M. Saleem, M. I. Khan, S. U. Khan, and Y. M. Chu, "Irreversibility analysis in natural bio-convective flow of Eyring-Powell nanofluid subject to activation energy and gyrotactic microorganisms," Ain Shams Engineering Journal, vol. 12, pp. 4063-4074, Dec. 2021, https://doi.org/10.1016/j.asej.2021.03.016.
[18]T. Thumma, S. R. Mishra, M. A. Abbas, M. M. Bhatti, and S. I. Abdelsalam, “Three-dimensional nanofluid stirring with non-uniform heat source/sink through an elongated sheet,” Applied Mathematics and Computation, vol. 421, p. 126927, May 2022, doi: 10.1016/j.amc.2022.126927.
[19]K. A. M. Alharbi et al., “Numerical solution of Maxwell-Sutterby nanofluid flow inside a stretching sheet with thermal radiation, exponential heat source/sink, and bioconvection,” International Journal of Thermofluids, vol. 18, p. 100339, May 2023, doi: 10.1016/j.ijft.2023.100339.
[20]R. Naveen Kumar, H. B. Mallikarjuna, N. Tigalappa, R. J. Punith Gowda, and D. Umrao Sarwe, “Carbon nanotubes suspended dusty nanofluid flow over stretching porous rotating disk with non-uniform heat source/sink,” International Journal for Computational Methods in Engineering Science and Mechanics, vol. 23, no. 2, pp. 119–128, Mar. 2022, doi: 10.1080/15502287.2021.1920645.
[21]V. K. R. S et al., “Analyzing magnetic dipole impact in fluid flow with endothermic/exothermic reactions: neural network simulation,” Phys. Scr., vol. 99, no. 6, p. 065215, May 2024, doi: 10.1088/1402-4896/ad4072.
[22]R. Kodi and O. Mopuri, “Unsteady MHD oscillatory Casson fluid flow past an inclined vertical porous plate in the presence of chemical reaction with heat absorption and Soret effects,” Heat Transfer, vol. 51, no. 1, pp. 733–752, 2022, doi: 10.1002/htj.22327.
[23]K. Karthik et al., “Computational examination of heat and mass transfer of nanofluid flow across an inclined cylinder with endothermic/exothermic chemical reaction,” Case Studies in Thermal Engineering, vol. 57, p. 104336, May 2024, doi: 10.1016/j.csite.2024.104336.
[24]A. Saeed, E. A. Algehyne, M. S. Aldhabani, A. Dawar, P. Kumam, and W. Kumam, “Mixed convective flow of a magnetohydrodynamic Casson fluid through a permeable stretching sheet with first-order chemical reaction,” PLOS ONE, vol. 17, no. 4, p. e0265238, Apr. 2022, doi: 10.1371/journal.pone.0265238.
[25]M. J et al., “Role of catalytic reactions in a flow-induced due to outer stationary and inner stretched coaxial cylinders: An application of Probabilists’ Hermite collocation method,” Case Studies in Thermal Engineering, vol. 56, p. 104218, Apr. 2024, doi: 10.1016/j.csite.2024.104218.
[26]P. Srilatha, R. S. V. Kumar, R. N. Kumar, R. J. P. Gowda, A. Abdulrahman, and B. C. Prasannakumara, “Impact of solid-fluid interfacial layer and nanoparticle diameter on Maxwell nanofluid flow subjected to variable thermal conductivity and uniform magnetic field,” Heliyon, vol. 9, no. 11, Nov. 2023, doi: 10.1016/j.heliyon.2023.e21189.
[27]N. Fatima et al., “Three-dimensional analysis of motile-microorganism and heat transportation of viscoelastic nanofluid with nth order chemical reaction subject to variable thermal conductivity,” Case Studies in Thermal Engineering, vol. 45, p. 102896, May 2023, doi: 10.1016/j.csite.2023.102896.
[28]G. Mandal and D. Pal, “Dual solutions of radiative Ag-MoS_2/water hybrid nanofluid flow with variable viscosity and variable thermal conductivity along an exponentially shrinking permeable Riga surface: Stability and entropy generation analysis,” International Journal of Modelling and Simulation, vol. 0, no. 0, pp. 1–26, doi: 10.1080/02286203.2023.2171656.
[29]M. Awais, T. Salahuddin, and S. Muhammad, “Effects of viscous dissipation and activation energy for the MHD Eyring-powell fluid flow with Darcy-Forchheimer and variable fluid properties,” Ain Shams Engineering Journal, vol. 15, no. 2, p. 102422, Feb. 2024, doi: 10.1016/j.asej.2023.102422.
[30]R. Kodi et al., “Influence of MHD mixed convection flow for maxwell nanofluid through a vertical cone with porous material in the existence of variable heat conductivity and diffusion,” Case Studies in Thermal Engineering, vol. 44, p. 102875, Apr. 2023, doi: 10.1016/j.csite.2023.102875.
[31]S. Liao, Homotopy Analysis Method in Nonlinear Differential Equations. Berlin, Heidelberg: Springer, 2012. doi: 10.1007/978-3-642-25132-0.
[32]J. Sui, L. Zheng, X. Zhang, and G. Chen, “Mixed convection heat transfer in power law fluids over a moving conveyor along an inclined plate,” International Journal of Heat and Mass Transfer, vol. 85, pp. 1023–1033, Jun. 2015, doi: 10.1016/j.ijheatmasstransfer.2015.02.014.
[33]Y. X. Li, H. Waqas, K. Al-Khaled, S. A. Khan, M. I. Khan, S. U. Khan, R. Naseem, and Y. M. Chu, "Simultaneous features of Wu's slip, nonlinear thermal radiation and activation energy in unsteady bio-convective flow of Maxwell nanofluid configured by a stretching cylinder," Chinese Journal of Physics, vol. 73, pp. 462-478, Oct. 2021, https://doi.org/10.1016/j.cjph.2021.07.033.
[34]S. Han, L. Zheng, C. Li, and X. Zhang, “Coupled flow and heat transfer in viscoelastic fluid with Cattaneo–Christov heat flux model,” Applied Mathematics Letters, vol. 38, pp. 87–93, Dec. 2014, doi: 10.1016/j.aml.2014.07.013.
[35]F. Haq, M. I. Khan, E. R. M. El-Zahar, S. U. Khan, S. Farooq, and K. Guedri, "Theoretical investigation of radiative viscous hybrid nanofluid towards a permeable surface of cylinder," Chinese Journal of Physics, vol. 77, pp. 2761-2772, June 2022, https://doi.org/10.1016/j.cjph.2022.05.013.
[36]W. Kuang, H. Wang, X. Li, J. Zhang, Q. Zhou, and Y. Zhao, "Application of the thermodynamic extremal principle to diffusion-controlled phase transformations in Fe-C-X alloys: Modeling and applications, " Acta Materialia, vol. 159, pp. 16-30, Oct. 2018, https://doi.org/10.1016/j.actamat.2018.08.008.
[37]S. P. A. Devi and M. Prakash, "Temperature dependent viscosity and thermal conductivity effects on hydromagnetic flow over a slendering stretching sheet," Journal of the Nigerian Mathematical Society, vol. 34, no. 3, pp. 318--330, Dec. 2015, doi: 10.1016/j.jnnms.2015.07.002.

International Journal of Engineering Research & Technology (IJERT)
ISSN: 2278-0181
Vol. 13 Issue 9, September 2024

[38]S. U. Khan, Usman, K. Al-Khaled, S. M. Hussain, A. Ghaffari, M. I. Khan, and A. W. Ahmed, "Implication of Arrhenius activation energy and temperature-dependent viscosity on non-Newtonian nanomaterial bio-convective flow with partial slip", Arabian Journal for Science and Engineering, vol. 47, pp. 7559-7570, Oct. 2021, https://doi.org/10.1007/s13369-021-06274-3.

[39]L. Sun, G. Wang, and C. Zhang, "Experimental investigation of a novel high performance multi-walled carbon nano-polyvinylpyrrolidone/silicon-based shear thickening fluid damper, Journal of Intelligent Material Systems and Structures," vol. 35, pp. 661-672, Feb. 2024, doi: 10.1177/1045389X231222999.

[40]. S. Mukhopadhyay and G. C. Layek, "Effects of thermal radiation and variable fluid viscosity on free convective flow and heat transfer past a porous stretching surface," International Journal of Heat and Mass Transfer, vol. 51, no. 9, pp. 2167--2178, May 2008, doi: 10.1016/j.ijheatmasstransfer.2007.11.038.

[41]W. Alhejaili, R. S. V. Kumar, E. R. El-Zahar, G. Sowmya, B. C. Prasannakumara, M. I. Khan, K. M. Yogeesha, and S. Qayyum, "Analytical solution for temperature equation of a fin problem with variable temperature-dependent thermal properties: Application of LSM and DTM-Pade approximant," Chemical Physics Letters, vol. 793, Articlr No. 139409, April 2022, https://doi.org/10.1016/j.cplett.2022.139409.

[42]Z. Wang, Q. Zhao, Z. Yang, R. Liang, and Z. Li, "High-speed photography and particle image velocimetry of cavitation in a Venturi tube," Physics of Fluids, vol. 36, Article No. 045147, April 2024, https://doi.org/10.1063/5.0203411.

[43]L. Miao and M. Massoudi, “Heat transfer analysis and flow of a slag-type fluid: Effects of variable thermal conductivity and viscosity,” International Journal of Non-Linear Mechanics, vol. 76, pp. 8–19, Nov. 2015, doi: 10.1016/j.ijnonlinmec.2015.05.001.

[44]Y. Fu, B. Bian, Y. Liu, L. Zhang, M. Li, J. Wen, and G. Xu, "Airside heat transfer analysis using Wilson plot method of three analogous serpentine tube heat exchangers for aero-engine cooling," Applied Thermal Engineering, vol. 248, Article No. 123238, July 2024, https://doi.org/10.1016/j.applthermaleng.2024.123238.

[45]G. Sulochana, C. V. Prasad, S. K. Bhatti, V. V. V. Madhav, K. K. Saxena, M. I. Khan, Z. Aloui, C. Prakash, and M. I. Khan, “Impact of multi-walled carbon nanotubes (MWCNTs) on hybrid biodiesel blends for cleaner combustion in CI engines,” Energy, vol. 303, Article No. 131911, Sep. 2024, https://doi.org/10.1016/j.energy.2024.131911.

[46]Y. Hou, M. Cheng, Z. Sheng, and J. Wang, “Unsteady conjugate heat transfer simulation of wall heat loads for rotating detonation combustor,” International Journal of Heat and Mass Transfer, vol. 221, Article No. 125081, April 2024, https://doi.org/10.1016/j.ijheatmasstransfer.2023.125081.

[47]Y. Zhang, M. Cheng, X. Liu, G. Rong, Z. Sheng, D. Shen, and J. Wang, “The influence of plug nozzle and Laval nozzle on the flow field and performance of non-premixed rotating detonation combustor,” Physics of Fluids, vol. 36, Article No. 056107, April 2024, https://doi.org/10.1063/5.0207508.